Optimization of cryogenic nitrogen rejection process with rejected nitrogen utilization

Mahdi Mostafavi, Saeed Eini*, Fatola Farhadi

Chemical and Petroleum Engineering Department, Sharif University of Technology, Tehran, Iran

* Corresponding author.
E-mail address: saeed.eini@sharif.edu (S. Eini)

Abstract

Nitrogen rejection from high-nitrogen natural gas (NG) streams is energy-intensive and reduces the economic viability of such resources. Various nitrogen rejection technologies have been developed to address this issue. This study presents a comprehensive economic evaluation of two cryogenic nitrogen rejection unit (NRU) configurations: single-column and double-column. The research introduces an economic enhancement by incorporating the rejected nitrogen into the value chain, proposing its use in enhanced oil recovery (EOR) instead of atmospheric venting. For this purpose, a compression-injection unit is integrated into the process. The evaluation considers four scenarios (two NRU configurations and two nitrogen utilization options) and uses net present value (NPV) as the optimization objective. Simulation and optimization results show that the double-column configuration is the most profitable when nitrogen is vented, with NPVs of $894 million and $1,073 million for single- and double-column configurations, respectively. However, when nitrogen is utilized for EOR, NPVs increase significantly to $4,787 million and $4,861 million, respectively. The economic advantage of the double-column configuration diminishes in the EOR case due to higher compression costs, highlighting that the optimal choice is context-dependent, as the single-column configuration becomes more profitable at increased EOR throughputs.

Keywords: High-nitrogen natural gas; Nitrogen rejection unit; Enhanced oil recovery; Economic evaluation; Optimization

1. Introduction

Natural gas (NG), owing to its widespread availability and lower emissions, is expected to see increased demand outpacing other fossil fuels [1,2]. Consequently, attention is shifting toward exploiting low-quality natural gas (NG) reserves, which contain higher levels of non-hydrocarbon components [3–5]. Notably, nitrogen constitutes approximately 57% of the contaminants in such reserves [6], and around 15% of the world's non-associated gas reserves fall into the high-nitrogen category [7]. High-nitrogen reservoirs are present in regions such as the US Mid-Continent, North Sea, Western Poland, and Southeast Asia [7,8]. In Iran, the Kabir Kuh, Samand, and Holeylan fields are notable for elevated nitrogen content [9].

High nitrogen levels diminish NG's calorific value and commercial appeal, while also increasing the size and cost of processing infrastructure [10,11]. To meet pipeline specifications, nitrogen content in NG must be reduced to below 4 mol% [7,12], typically through nitrogen rejection units (NRUs). A range of nitrogen separation technologies exists including cryogenic distillation, pressure swing adsorption, absorption, and membrane separation [13]. Although both adsorption and cryogenic distillation have been well studied, the latter is widely used industrially due to its benefits [10,14,15]. This method benefits from economies of scale [16] and is compatible with other cryogenic NG processing units like LNG production [17,18] and helium recovery [19,20]. Cryogenic distillation's additional merits include its independence from proprietary solvents or adsorbents and its superior separation efficiency, which enables methane recoveries above 98% and high nitrogen purity [4]. In venting scenarios, it is often the only option capable of limiting methane emissions to environmentally acceptable levels. However, the process is energy-intensive, which necessitates efficiency optimization.

MacKenzie et al. [21] analyzed power requirements for various NRU configurations across different feed compositions but did not address optimal process conditions. Hamedi et al. [8] focused on minimizing energy consumption in different cryogenic setups considering variable nitrogen content but also did not optimize process economics. Recent works have also evaluated cryogenic NRUs with respect to CO_2 tolerance [22–24], though Spatolisano and Pellegrini [24] focused more on comparative thermodynamic performance than economic viability. However, by treating the NRU as a standalone unit focused on internal efficiency, these studies have largely overlooked the crucial economic interplay between the separation process and the downstream value of the rejected nitrogen.

Given the high operating costs of developing high-nitrogen NG reserves, a practical route to improving economic attractiveness lies in repurposing the rejected nitrogen. This study proposes utilizing the nitrogen byproduct for enhanced oil recovery (EOR) instead of atmospheric venting. Nitrogen injection, a proven EOR method, is attractive due to nitrogen's inertness, non-corrosiveness, and high formation volume factor.

The main contribution of this work lies in addressing this gap through an integrated techno-economic optimization framework. We model and optimize a complete system, from the NRU inlet, through compression and transport, to the revenue generated by EOR. This integrated approach enables a direct and rigorous comparison of the two process configurations studied (single-column and double-column) under distinct nitrogen handling scenarios (venting scenario and EOR scenario). This comparison is crucial, as the optimal NRU configuration may be highly dependent on the chosen downstream objective for the rejected nitrogen. This allows us to determine the optimal design based on overall profitability, providing a more comprehensive perspective than found in prior literature. A nitrogen compression-injection system is integrated in the EOR scenarios to assess the full economic impact. The process flowsheets are simulated and optimized using net present value (NPV) over a 25-year project life as the primary performance metric.

In Section 2, the problem is formulated, and the NRU configurations and nitrogen injection unit are presented and described. The optimization procedure is discussed in Section 3, where the decision variables and objective function formulation are detailed. Finally, in Section 4, the comparative results are depicted and discussed in order to conclude the effect of adding nitrogen utilization to the economics of NRUs.

2. Problem statement

This study aims to optimize and evaluate the nitrogen rejection process for a high-nitrogen NG stream. The produced low-nitrogen NG should meet the pipeline specifications. The NRU feed and product specifications are shown in Table 1. In this study, the NRU feed is considered a binary mixture of CH_4 and N_2, which is a reasonable assumption. Impurities like CO_2, water, and C_{2+} are necessarily removed in upstream pre-treatment units, as their presence would lead to freezing at the cryogenic temperatures required for the process.

This study involves the evaluation and comparison of two NRU configurations, which are described in the following sections.

2.1. Single-column configuration

The single-column process configuration [7] utilizes a closed-loop methane-based heat pump connected to a high-pressure (HP) distillation column (Figure 1). The heat pump working fluid is compressed using a multi-stage compressor (K-3) to supply heat to the reboiler (E-6), then condensed and vaporized in the condenser (E-5) at near-atmospheric pressure to create column reflux. Feed gas enters the system at 60 bar, is pre-cooled by the column's product streams, and then throttled via Joule-Thomson valve JT1 to the operating pressure of 21–28 bar for the HP column. The column separates the gas into a nitrogen-rich top stream and a methane-rich bottom stream. The low-pressure (LP) methane-rich gas (stream 6) is then recompressed to meet pipeline delivery standards, while the nitrogen-rich stream (stream 9) exits at pressures typically above 21 bar.

This configuration is advantageous due to its ability to handle varying nitrogen concentrations in feed gas and produce high-purity products. However, its drawbacks include high energy consumption [7,25,26].

2.2. Double-column configuration

The double-column process configuration [7] consists of two vertically stacked distillation columns, with the lower column operating at higher pressure than the upper one (Figure 2). Feed gas is first partially liquefied in multi-stream heat exchanger E-1, then depressurized through valve JT1 to match the HP column's operating pressure (21–28 bar). The HP and LP columns are thermally integrated via heat exchanger E-4, embedded within the column system.

The HP column's bottom product, a CH_4-N_2 mixture, is cooled (E-2), expanded (JT3), and introduced into the LP column at near-atmospheric pressure [27]. Final separation occurs in the LP column, producing a nitrogen-rich gas at the top and a methane-rich liquid at the bottom.

For effective operation without external refrigeration, the feed gas must contain at least 25–30 mol% nitrogen [7,25–27]; lower nitrogen levels may reduce methane recovery or hinder process feasibility. Nonetheless, this configuration remains adaptable to varying nitrogen contents [3]. Its thermally integrated design enhances energy efficiency, translating into notable cost savings and making it an economically favorable option.

2.3. Nitrogen Injection

In cryogenic nitrogen rejection processes, rejected nitrogen, which is warmed to near ambient temperature by cooling hot process streams, is often vented to the atmosphere. However, this study proposes using nitrogen as an enhanced oil recovery (EOR) agent instead. Nitrogen is ideal for EOR due to its abundance, inertness, non-corrosiveness, non-flammability, low compressibility, and high formation volume factor [28–31].

To utilize nitrogen for EOR, it must be transported via pipeline to oil fields and compressed to the required injection pressure using multi-stage centrifugal compressors with intercoolers and aftercoolers, as shown in Figure 3. While this approach introduces additional costs, including transportation, compression, well development, and oil production, it significantly boosts oil recovery, thereby enhancing overall project revenues.

Considering the NRU configurations and potential nitrogen pathways, four scenarios are simulated and optimized in order to provide an optimal solution (Figure 4):

- Single-column configuration ~~and releasing nitrogen into the atmosphere~~ (SC-N_2-Vent)
- Single-column configuration and utilization of rejected nitrogen in the EOR process (SC-N_2-EOR)
- Double-column configuration and releasing nitrogen into the atmosphere (DC-N_2-Vent)
- Double-column configuration and utilization of rejected nitrogen in the EOR process (DC-N_2-EOR)

2.4. Process design data

To meet pipeline specifications, the NRU reduces nitrogen content in the feed gas to below 4 mol% [7,12]. Table 2 presents the relevant design data and process specifications.

For a fair comparison between the SC-N_2-EOR and DC-N_2-EOR scenarios, it is assumed that both configurations result in the same oil recovery (30,000 barrels per day). A natural gas (NG) processing unit is located near the gas field, with nitrogen transported 300 km via an onshore pipeline to the oil field. The EOR injection pressure is set at 300 bar, and injection wells are drilled to a depth of 3,000 meters. The number of wells required is determined based on the nitrogen injection rate, with a single well assumed to handle 0.3 MMSCMD, the midpoint of the 0.2-0.4 MMSCMD capacity range reported in literature [32].

A key parameter in the economic evaluation of gas injection-based EOR is "η_{InjGas}", which represents the volume of injection gas required to produce one barrel of oil. Although this value can vary depending on field characteristics, typical ranges are well-documented. For nitrogen, η_{InjGas} is assumed to be 70 SCM N_2/bbl oil in this study, which aligns with reported values. This assumption facilitates consistent analysis across both configurations and enables accurate estimation of oil production and associated economic outcomes. Comparative data for CO_2-based injection is also included in Table 3 for reference.

3. Process simulation and optimization procedure

This section discusses the optimization algorithm, decision variables, constraints, and objective function used in this research.

3.1. Simulation software and optimization algorithm

The scenarios are simulated in Aspen HYSYS V10 using the Peng-Robinson (PR) equation of state (EoS), which has been shown to provide the most accurate results for cryogenic NRU simulations compared to alternatives like SRK and PRSV [33]. Optimization is performed using a genetic algorithm (GA) implemented in MATLAB and connected to HYSYS via ActiveX. Metaheuristic methods like GA are well-suited for complex, non-linear optimization problems, especially when objective functions are evaluated through external simulators [34–36]. The GA tuning parameters are detailed in Table 4, and the overall optimization procedure is illustrated in Figure 5.

3.2. Decision variables

The decision variables used in the optimization of both process configurations encompass the temperatures and pressures of the streams. For the single-column process, the flow rates of methane and nitrogen in the heat pump working fluid are also decision variables. Tables 5 and 6 present the decision variables along with their respective lower and upper bounds for the single-column and double-column configurations, respectively.

3.3. Objective function and constraints

In this study, flowsheets are optimized using NPV as the objective function over a specific project lifetime. In the optimization process, the goal is to maximize the NPV, which is equivalent to minimizing its negative value. NPV is calculated using the following equation:

$$NPV_n = \sum_{t=0}^{n} \frac{NCF_t}{(1+r)^t} \tag{1}$$

where NCF_t is the net cash flow (revenues minus costs) in the t-th year, r is the discount rate, and n is the life of the project [37]. The economic analysis is performed considering a discount rate of 15% over a 25-year time horizon (r = 0.15, n = 25), and it is assumed that the plant operates for 8,000 hours (333 days) per year.

Revenues are derived from selling processed natural gas and additional oil recovered through EOR, with fixed prices of $75 per barrel of oil and $0.35 per SCM of gas in the reference scenario. Annual natural gas treatment costs include two components: (1) feed gas cost, estimated at $0.05 per SCM of high-nitrogen gas which is slightly above conventional rates to account for the reservoir's complexity; and (2) the total annual cost (TAC) of the NRU process, which includes annualized capital expenditure (CAPEX) and operating expenditure (OPEX). The methods for economic analysis are detailed in Section 3.4 and the Supplementary data (Appendix A, Sections A.1–A.9).

It is assumed that the maximum acceptable N_2 content in the sales gas is 4 mol% [7,12].

$$x_{N_2}^{Bot} \leq 0.04 \tag{2}$$

To minimize methane loss and ensure flexibility, the CH_4 concentration in the rejected N_2 stream is limited to below 1 mol% [25,38], regardless of whether nitrogen is vented or used for EOR.

$$x_{CH_4}^{Top} \leq 0.01 \tag{3}$$

The minimum temperature approach (*MTA*) is assumed to be 2 ℃ in all the MSHEs.

$$MTA_{MSHE} \geq 2\,^{\circ}C \tag{4}$$

The degree of superheating at the suction side of the compressors must be greater than 10 ℃ in order to prevent the formation of liquid phase in the compressors.

$$T_{in}^{Comp} - T_{dew}^{Comp} \geq 10\,^{\circ}C \tag{5}$$

The compressors are limited to a maximum compression ratio (*CR*) of 5 (the maximum allowable compression ratio of a typical commercial compressor is about 4 to 5 [39,40]). Higher compression ratios can lead to decreased efficiency and higher discharge temperatures, which can intensify mechanical stress problems.

$$CR \leq 5 \tag{6}$$

If there are process modules in the simulation that fail to converge, the penalty function will be determined based on the number of non-converged modules (N_{NC}).

$$Pen_{NC} = 10^{Max\{0,\,5N_{NC}\}} \tag{7}$$

If the minimum temperature approach of the MSHEs is less than 2 ℃, the penalty function will be calculated using Eq. (5). It is worth mentioning that Aspen HYSYS will display a negative value when a temperature cross occurs.

$$Pen_{TC} = 10^{Max\{0,\,2-MTA_{MSHE}\}} \tag{8}$$

If the degree of superheating at the suction side of the compressor falls below the set value of 10 ℃, the penalty function is as follows:

$$Pen_{DoS} = 10^{Max\left\{10-\left(T_{in}^{Comp}-T_{dew}^{Comp}\right)\right\}} \tag{9}$$

In the double-column configuration, thermal coupling between the HP and LP columns eliminates the LP column's degree of freedom, making it impossible to independently specify component concentrations in its output. As the LP column converges through this link, specific penalty functions are applied to account for constraint handling in the optimization process:

$$Pen_{N_2}^{DC} = 10^{Max\left\{0,\,100\left(x_{N_2}^{Bot}-0.04\right)\right\}} \tag{10}$$

$$Pen_{CH_4}^{DC} = 10^{Max\left\{0,\,100\left(x_{CH_4}^{Top}-0.01\right)\right\}} \tag{11}$$

3.4. Cost estimation

Evaluating the objective function requires estimating the capital and operating costs for all major equipment. When direct cost relationships are unavailable or overly complex, simplified formulas are used such as estimating operating costs as a percentage of capital costs. All economic evaluations are based on 2023 data.

NRU costs

For both single- and double-column NRU configurations, key equipment includes multi-stream heat exchangers, intercoolers, HP and LP columns (shell and trays), and multi-stage compressors. Joule-Thomson valves are excluded from cost estimation. Cost estimation methods for all process equipment are detailed in the Supplementary data (Appendix A, Sections A.1–A.5).

Transportation costs

Nitrogen gas can be transported via pipeline, truck, rail, or ship, but the latter three often require a phase change. Due to its maturity and cost-effectiveness, pipeline transport is selected for this

study. Transport cost depends heavily on distance and volume (see Supplementary data, Appendix A, Section A.7). Total Annual Cost (TAC) includes capital and operating costs. Capital costs comprise materials, installation, and control stations. Operating and maintenance costs are assumed to be 4% of capital costs [41].

Gas injection costs

Costs for nitrogen injection in EOR are calculated from compression equipment, injection wells, and oil recovery expenses. Cost correlations for the compressors and wells are provided in the Supplementary data (Appendix A, Section A.8). Oil extraction costs are assumed at $10 per barrel [42]. Water injection is not considered. Operating costs for injection cover compressor energy use and 4% of injection well capital costs [43].

Utility costs

Electricity and cooling water costs are estimated at $0.083/kWh [44] and $0.025/m^3 [45], respectively. Calculation procedures are available in the Supplementary data (Appendix A, Sections A.6 and A.9).

4. Results and discussion

4.1. Techno-economic analysis

The scenarios described in section 2.3 were optimized using the method in Section 3.1, with 13 and 9 decision variables for the single- and double-column configurations, respectively. Tables 7 and 8 show the optimal values.

Figure 6 compares CAPEX, OPEX, TAC, and NPV_{25} across scenarios. While N_2-EOR scenarios incur significantly higher costs due to nitrogen transportation and injection, they also yield substantially more revenue from increased oil production. As a result, the NPV_{25} for SC-N_2-EOR and DC-N_2-EOR scenarios exceeds that of SC-N_2-Vent and DC-N_2-Vent, indicating that profitability in nitrogen injection scenarios is largely driven by oil sales, despite higher operational expenses.

As shown in Figure 6, the DC-N_2-Vent scenario has the lowest capital, operating, and total annual costs. Its operating costs and TAC are about one-third of those in the SC-N_2-Vent scenario. This cost advantage stems from fundamental design differences between the two configurations. Unlike the single-column setup, the double-column configuration relies on thermal integration rather than external refrigeration to handle condenser and reboiler duties. This eliminates the need for

additional multi-stage compressors and heat exchangers used in the single-column's heat pump system. Since compressor power consumption significantly contributes to operating costs, removing the heat pump results in notable cost savings. As a result, the DC-N_2-Vent scenario achieves a higher NPV_{25} compared to SC-N_2-Vent.

Figure 7 illustrates the capital cost distribution for installed equipment across different scenarios. In nitrogen venting scenarios (Figures 7.a and 7.b), compressors represent the largest capital expense. Conversely, in nitrogen injection scenarios (Figures 7.c and 7.d), pipeline costs account for over 50% of capital expenditures, indicating that transportation efficiency greatly affects overall project profitability.

In both SC-N_2-Vent and SC-N_2-EOR scenarios, the cost of heat pump compressors exceeds that of compressors used for sales gas compression or nitrogen injection. This is due to the high compression ratio required in the heat pump system. The working fluid is first reduced to about 1.5 bar before the evaporator (E-5) and then raised to 30 bar before the condenser (E-6), requiring a two-stage compressor with a compression ratio of ~20 and a high flow rate.

For nitrogen injection, based on the assumption that 70 SCM of nitrogen is needed to produce one barrel of oil, recovering 30,000 barrels per day requires injecting 2.1 MMSCMD of nitrogen. With each injection well handling 0.3 MMSCMD, seven wells are needed, costing an estimated $28.8 million for drilling.

Figure 8 presents a comparative diagram of power consumption in different scenarios. The diagram is divided into two subsections: (i) power consumption of the NRU per MMSCMD of feed gas, and (ii) power consumption of nitrogen injection per MMSCMD of nitrogen. The graph clearly illustrates that in the DC-N_2-EOR scenario, the highest power consumption is related to the gas injection process. In fact, the power requirement for gas injection in the DC-N_2-EOR scenario is roughly two times higher than that in the SC-N_2-EOR scenario when considering the recovery of a specific quantity of crude oil. The main reason for this difference is that the nitrogen injection compressors used in the double-column configuration must provide a higher overall compression ratio than those utilized in the single-column process. The double-column configuration produces nitrogen gas at a lower pressure (1.62 bar) compared to the single-column configuration (26.40 bar). Consequently, in order to increase the nitrogen pressure to the injection pressure of 300 bar, the compressors in the single-column and double-column configurations must provide overall compression ratios of 11.4 and 185.2, respectively, with the former incurring higher costs.

For the SC-N_2-EOR scenario, the total power consumption (sum of the power required for the sales gas compression and nitrogen injection) per unit flow rate of feed is 5,575 kW, whereas for the DC-N_2-EOR scenario, it is 4,595 kW. Despite the need for a higher overall compression ratio and the subsequent increase in power consumption for nitrogen gas injection in the DC-N_2-EOR scenario, the total power consumption is higher in the SC-N_2-EOR scenario. As previously discussed, the main reason for this is the extremely high power consumption observed in the heat pump in the single-column process.

To investigate the key parameters and their influence on the performance of each process configuration, a sensitivity analysis was performed in this study. The specific analyses carried out include:

- Effect of oil production volume on NPV_{25} and TAC_{unit}
- Effect of electricity price on NPV_{25} and TAC_{unit}
- Effect of sales gas price on NPV_{25}
- Effect of feed flow rate on NPV_{25} and TAC_{unit}
- Effect of η_{InjGas} on NPV_{25}

The influence of the number of additional oil barrels produced through nitrogen injection on the NPV_{25} and TAC_{unit} is presented in Figures 9 and 10, respectively. TAC_{unit} represents the total annual costs associated with the NRU, gas transmission, and gas injection. It does not include the costs of feed gas and oil production. Figure 9 clearly indicates that the NPV_{25} is significantly affected by the number of additional barrels of oil produced. Notably, an increase of one barrel in oil production leads to an increase in NPV_{25} of approximately $135,000. Moreover, as the crude oil production continues to rise, the difference in both the NPV_{25} and TAC_{unit} between the SC-N_2-EOR and DC-N_2-EOR scenarios decreases, as seen in Figures 9 and 10. This trend persists until the oil recovery reaches approximately 56,000 barrels per day, at which point the NPV_{25} and TAC_{unit} become equal for both scenarios, rendering them equally favorable options. The primary cause for this can be attributed to the nitrogen injection compressors. When oil production increases, there is a corresponding increase in the amount of injected gas. On the other hand, double-column process compressors must provide a higher overall compression ratio for injection, resulting in a more pronounced rate of change of power consumption with respect to the nitrogen flow rate. As a result, as oil production exceeds 56,000, the costs of the DC-N_2-EOR scenario

become higher than those of the SC-N_2-EOR scenario. Hence, for oil productions above 56,000 barrels per day, the single-column configuration proves to be an economically viable option, while for oil productions below 56,000 barrels per day, the double-column configuration is recommended. It is worth highlighting that, in this particular case, the maximum oil recovery is limited to 62,000 barrels per day. This upper limit is determined by considering both the maximum flow rate of nitrogen gas produced by the process and the parameter η_{InjGas}.

Figure 11 provides a magnified view, specifically focusing on the precise intersection point between the NPV_{25} curves displayed in Figure 9. Figure 11 illustrates that for the SC-N_2-EOR and DC-N_2-EOR scenarios to achieve an equal NPV_{25} value as their corresponding scenarios where nitrogen gas is released into the atmosphere (SC-N_2-Vent and DC-N_2-Vent scenarios), the minimum oil production levels need to be around 1,570 and 1,700 barrels per day, respectively. In simpler terms, these data points indicate the specific oil production levels required to offset the costs associated with gas transmission and injection in the SC-N_2-EOR and DC-N_2-EOR scenarios. Furthermore, the SC-N_2-EOR and DC-N_2-EOR scenarios need to maintain an oil recovery rate of approximately 2,870 and 1,700 barrels per day, respectively, to achieve equal NPV_{25} values with the DC-N_2-Vent scenario, which demonstrates the highest NPV_{25} when nitrogen is vented.

Figure 12 illustrates the impact of the sales gas price on the NPV_{25} in different scenarios. Despite a decrease in the sales gas price to 10 cents per SCM, or even lower, the NPV_{25} remains positive in the SC-N_2-EOR and DC-N_2-EOR scenarios due to the substantial revenue generated from oil sales, but in the SC-N_2-Vent and DC-N_2-Vent scenarios, the NPV_{25} turns negative. For NPV_{25} to remain positive in the SC-N_2-Vent and DC-N_2-Vent scenarios, the sales gas prices must be higher than \$0.18 and \$0.15 per SCM, respectively.

Figure 13 shows the variations of the NPV_{25} and TAC_{unit} with electricity prices for the SC-N_2-Vent and DC-N_2-Vent scenarios. Considering the fact that the single-column configuration has a higher power consumption than the double-column configuration, the slopes of the NPV_{25} and TAC_{unit} curves of the single-column configuration (SC-N_2-Vent) are steeper. As shown in Figure 13, the double-column configuration becomes a more suitable option at higher electricity prices due to its lower power consumption. Unlike the single-column configuration, the double-column configuration is less affected by changes in electricity prices. As the electricity price rises from \$0.04/kWh to \$0.16/kWh, the TAC_{unit} for the DC-N_2-Vent scenario increases by about 113% (from

$8.3 M to $17.7 M), whereas for the SC-N_2-Vent scenario, it rises by approximately 139% (from $22.2 M to $53.1 M).

The changes in NPV_{25} with respect to electricity prices are not as significant as the changes in costs, primarily because the NPV_{25} is more sensitive to the revenue generated from product sales than costs. When the electricity price increases from $0.04/kWh to $0.16/kWh, the NPV_{25} in the DC-N_2-Vent scenario experiences a decrease of approximately 5.5% (from $1.09 billion to $1.03 billion). Similarly, in the SC-N_2-Vent scenario, the NPV_{25} decreases by approximately 20.8% (from $0.96 billion to $0.76 billion). It should be noted that the SC-N_2-EOR and DC-N_2-EOR scenarios are expected to exhibit similar behavior to the SC-N_2-Vent and DC-N_2-Vent scenarios, respectively.

The analyses performed in this study were based on the assumption that injecting 70 SCM of nitrogen gas is necessary per barrel of oil recovery. Figure 14 illustrates the variation of the maximum achievable oil production and the corresponding NPV_{25} versus the parameter η_{InjGas}. As η_{InjGas} increases, the oil production decreases for a given quantity of the injection gas. Given that the revenue generated from oil sales significantly impacts the NPV_{25}, a decline in oil production leads to a substantial decrease in the NPV_{25}.

4.2 Preliminary Environmental Considerations

This section presents a screening-level comparison of greenhouse gas (GHG) emissions between the venting and EOR injection pathways. The objective is to evaluate the environmental trade-offs associated with different nitrogen-rejection strategies by integrating the mass and energy balance results from the preceding sections. The intent is to quantify the dominant contributors (methane slip vs. compression electricity) rather than to present a full life-cycle assessment result.

All calculations were performed from the simulation outputs summarized in Table 9. Direct methane CO_2e for venting was computed from the simulated CH_4 molar flow using GWP_{100} (fossil CH_4)=29.8 [46]. Indirect electricity emissions were estimated from simulated compression power using a grid emission factor; in the absence of site-specific data, the EPA eGRID U.S. average total-output rate (770.884 lbCO_2e/MWh) may be used as an illustrative default [47,48].

As shown in Table 9, venting yields a higher gate-to-gate footprint (≈2.12–2.18×10^5 tCO_2e/y) because it includes direct methane CO_2e (≈1.25–1.91×10^5 tCO_2e/y) in addition to power-related emissions. In contrast, under the stated gate-to-gate boundary, utilization for EOR avoids vent methane release, and the gate-to-gate footprint becomes electricity-driven (≈0.88–1.07×10^5

tCO_2e/y), reflecting the dominance of compression power in this route. Consequently, the comparative outcome is sensitive to the assumed grid emissions intensity and to any boundary expansion beyond the injection header (e.g., additional infrastructure, field operations, fugitives, or downstream system consequences). Therefore, conducting an ISO-consistent LCA with clearly defined boundaries is an essential next step to reliably compare and identify the most environmentally beneficial option.

5. Conclusions

This study evaluated and optimized single- and double-column cryogenic NRU configurations for nitrogen venting and EOR utilization scenarios. The results indicate that the double-column configuration is generally more profitable in the base case for both scenarios. Specifically, when venting nitrogen, the TAC of the double-column unit is approximately one-third of the single-column unit, significantly enhancing its NPV.

However, the economic superiority of the double-column configuration is highly sensitive to the scale of production. Due to its lower operating pressure, the compression costs for EOR increase more sharply than in the single-column unit. A critical crossover point was identified at an oil production rate of approximately 56,000 barrels per day; beyond this threshold, the single-column configuration becomes more economically advantageous due to its lower compression duties. Furthermore, the study highlights that while the double-column unit benefits from superior heat integration, the single-column unit's reliance on a heat pump makes it less competitive at smaller scales. From a screening-level gate-to-gate GHG perspective, venting is dominated by methane slip while the EOR pathway is dominated by compression electricity, leading to a lower footprint for EOR under the assumed boundary and grid intensity. Future work should perform a comprehensive LCA and quantitatively assess the environmental trade-offs between methane emissions and compression energy demands (including sensitivity to grid emissions intensity).

Supplementary data

Supplementary data is provided for this manuscript that contains the data and correlations required for economic evaluation.

Nomenclature

Abbreviations	
CAPEX	Capital Expenditure

EGR	Enhanced Gas Recovery
EOR	Enhanced Oil Recovery
EoS	Equation of State
GA	Genetic Algorithm
HEX	Heat Exchanger
HP	High-Pressure
LP	Low-Pressure
MMSCMD	Million Standard Cubic Meters per Day
MSHE	Multi-Stream Heat Exchanger
NG	Natural Gas
NPV	Net Present Value
NRU	Nitrogen Rejection Unit
OPEX	Operating Expenditure
PR	Peng-Robinson
PRSV	Peng-Robinson-Stryjek-Vera
SCM	Standard Cubic Meter
SRK	Soave-Redlich-Kwong
STHE	Shell and Tube Heat Exchanger
TEA	Techno-Economic Assessment
TAC	Total Annual Cost, $
CO2e	Carbon Dioxide Equivalent
GHG	Greenhouse Gas
GWP_{100}	Global Warming Potential over 100 years
SC-N_2-EOR	Single-column configuration and utilization of rejected nitrogen in the EOR process
SC-N_2-Vent	Single-column configuration and releasing nitrogen into the atmosphere
DC-N_2-EOR	Double-column configuration and utilization of rejected nitrogen in the EOR process
DC-N_2-Vent	Double-column configuration and releasing nitrogen into the atmosphere
Variables/Parameters	
CR	Compression ratio
MTA	Minimum temperature approach, ℃ or K
NCF	Net cash flow, $
NPV	Net present value, $
Pen	Penalty function
r	Discount rate
T	Temperature, ℃
x	Mole fraction
z	Decision variable
Subscripts	
CH_4	Methane
dew	Dew point

DoS	Degree of superheating
in	Inlet stream
InjGas	Injection gas
MSHE	Multi-stream heat exchanger
n	Project lifetime, year
N_2	Nitrogen
NC	Non-convergence
t	t-th year
TC	Temperature cross
Superscripts	
Bot	Bottom of column
Comp	Compressor
DC	Double-column
Top	Top of column
Greek letters	
η	The quantity of injection gas required to produce one barrel or a certain amount of oil, SCM

The Supplementary data is available at:

file:///C:/Users/pc/Downloads/Supplementary%20data-Dr.%20Eini.pdf

References

1. ExxonMobil, *ExxonMobil Global Outlook: Our View to 2050* (2025).
2. Yarlagadda, B., Iyer, G., Binsted, M., et al., "The future evolution of global natural gas trade", *iScience*, **27**(2), 108902 (2024). https://doi.org/10.1016/j.isci.2024.108902.
3. Kidnay, A. J., Parrish, W. R., and McCartney, D. G., *Fundamentals of Natural Gas Processing*, 3rd Edn., CRC Press, Boca Raton, FL, USA (2019).
4. Rufford, T. E., Smart, S., Watson, G. C. Y., et al., "The removal of CO_2 and N_2 from natural gas: A review of conventional and emerging process technologies", *Journal of Petroleum Science and Engineering*, **94**–**95**, pp. 123–154 (2012). https://doi.org/10.1016/j.petrol.2012.06.016.
5. Surmi, A., Shariff, A. M., and Lock, S. S. M., "Techno-economic assessment of cryogenic Rotating Packed Beds for nitrogen removal from natural gas", *Results in Engineering*, **26**, 104918 (2025). https://doi.org/10.1016/j.rineng.2025.104918.
6. Bradley Curtis III, A. and Wess, M., "Commercialization of Nitrogen-Rich Natural Gas", The University of Oklahoma (2008).
7. Mokhatab, S., Poe, W. A., and Mak, J. Y., *Handbook of Natural Gas Transmission and Processing: Principles and Practices*, 4th Edn., Gulf Professional Publishing, Oxford, UK (2019).

8. Hamedi, H., Karimi, I. A., and Gundersen, T., "Optimal cryogenic processes for nitrogen rejection from natural gas", *Computers & Chemical Engineering*, **112**, pp. 101–111 (2018). https://doi.org/10.1016/j.compchemeng.2018.02.006.

9. Bordenave, M. L., "The origin of the Permo-Triassic gas accumulations in the Iranian Zagros foldbelt and contiguous offshore areas: a review of the Palaeozoic petroleum system", *Journal of Petroleum Geology*, **31**(1), pp. 3–42 (2008). https://doi.org/10.1111/j.1747-5457.2008.00405.x.

10. Kuo, J. C., Wang, K. H., and Chen, C., "Pros and cons of different Nitrogen Removal Unit (NRU) technology", *Journal of Natural Gas Science and Engineering*, **7**, pp. 52–59 (2012). https://doi.org/10.1016/j.jngse.2012.02.004.

11. Guo, D. and Jiang, P., "Process analysis and optimization of high N2 natural gas liquefaction", *Process Safety and Environmental Protection*, **178**, pp. 1170–1177 (2023). https://doi.org/10.1016/j.psep.2023.08.021.

12. Lak, S. Z., Rostami, M., and Rahimpour, M. R., "Nitrogen separation from natural gas using absorption and cryogenic processes", In *Advances in Natural Gas: Formation, Processing, and Applications. Volume 5: Natural Gas Impurities and Condensate Removal*, M. R. Rahimpour, M. A. Makarem, and M. Meshksar (Eds.), Elsevier, pp. 185–200 (2024). https://doi.org/10.1016/B978-0-443-19223-4.00005-X.

13. Rao, F., Lu, Z., Guo, Y., et al., "The separation of methane and nitrogen in natural gas processing: A review", *Separation and Purification Technology*, **363**, 132107 (2025). https://doi.org/10.1016/j.seppur.2025.132107.

14. Zhou, Y., Yuan, Y., Cong, S., et al., "N2-selective adsorbents and membranes for natural gas purification", *Separation and Purification Technology*, **300**, 121808 (2022). https://doi.org/10.1016/j.seppur.2022.121808.

15. Khoramzadeh, E., Bakhtyari, A., and Mofarahi, M., "Nitrogen rejection from natural gas by adsorption processes and swing technologies", In *Advances in Natural Gas: Formation, Processing, and Applications. Volume 5: Natural Gas Impurities and Condensate Removal*, M. R. Rahimpour, M. A. Makarem, and M. Meshksar (Eds.), Elsevier, pp. 201–228 (2024). https://doi.org/10.1016/B978-0-443-19223-4.00008-5.

16. Arizmendi-Sanchez, J. and Finn, A., "Nitrogen removal for chemicals production", *PTQ Gas*, pp. 29–33 (2016).

17. Ghorbani, B., Zendehboudi, S., and Saady, N. M. C., "Advancing Hybrid Cryogenic Natural Gas Systems: A Comprehensive Review of Processes and Performance Optimization", *Energies*, **18**(6), 1443 (2025). https://doi.org/10.3390/en18061443.

18. Ebrahimi, A., Ghorbani, B., Skandarzadeh, F., et al., "Integrated LNG/NRU Configuration with the Biomass Gasification Unit and Absorption-Compression Refrigeration System", *Waste and Biomass Valorization*, **13**(3), pp. 1731–1748 (2022). https://doi.org/10.1007/s12649-021-01597-6.

19. Gao, P., Cong, C., Jiang, H., et al., "Advanced integration and optimization of cryogenic helium recovery in natural gas treatment plants", *Separation and Purification Technology*, **361**, 131547 (2025). https://doi.org/10.1016/j.seppur.2025.131547.

20. Jiang, H., Gao, P., and Li, H., "Optimization of co-production process of cryogenic helium concentration and liquefied natural gas", *Applied Thermal Engineering*, **225**, 120153 (2023). https://doi.org/10.1016/j.applthermaleng.2023.120153.

21. MacKenzie, D., Cheta, I., and Burns, D., "Removing nitrogen", *Hydrocarbon Engineering*, **7**(11),

pp. 57–63 (2002).

22. Farooq, A., Finn, A., Hosainy, A., et al., "Carbon dioxide tolerant nitrogen rejection reduces cost", *GPA Europe Annual Conference*, Florence, Italy (2015).

23. De Guido, G., Messinetti, F., and Spatolisano, E., "Cryogenic Nitrogen Rejection Schemes: Analysis of Their Tolerance to CO2", *Industrial & Engineering Chemistry Research*, **58**(37), pp. 17475–17488 (2019). https://doi.org/10.1021/acs.iecr.9b02544.

24. Spatolisano, E. and Pellegrini, L. A., "CO_2-Tolerant Cryogenic Nitrogen Rejection Schemes: Analysis of Their Performances", *Industrial & Engineering Chemistry Research*, **60**(11), pp. 4420–4429 (2021). https://doi.org/10.1021/acs.iecr.0c06189.

25. Mokhatab, S., Mak, J. Y., Valappil, J. V., et al., *Handbook of Liquefied Natural Gas*, Gulf Professional Publishing, Oxford, UK (2014).

26. Linde, *State-of-the-Art Nitrogen Rejection Technology: Increasing the Energy Density of Natural Gas* (2019).

27. Windmeier, C. and Barron, R. F., "Cryogenic Technology", *Ullmann's Encyclopedia of Industrial Chemistry*, pp. 1–71 (2013). https://doi.org/10.1002/14356007.b03_20.pub2.

28. Tileuberdi, N. and Gussenov, I., "Review on miscible, immiscible, and progressive nitrogen injection for enhanced oil recovery", *Energy Reports*, **12**, pp. 360–367 (2024). https://doi.org/10.1016/j.egyr.2024.06.004.

29. Mogensen, K. and Xu, S., "Comparison of three miscible injectants for a high-temperature, volatile oil reservoir - With particular emphasis on nitrogen injection", *Journal of Petroleum Science and Engineering*, **195**, 107616 (2020). https://doi.org/10.1016/j.petrol.2020.107616.

30. Zanganeh, P., Dashti, H., and Ayatollahi, S., "Comparing the effects of CH_4, CO_2, and N_2 injection on asphaltene precipitation and deposition at reservoir condition: A visual and modeling study", *Fuel*, **217**, pp. 633–641 (2018). https://doi.org/10.1016/j.fuel.2018.01.005.

31. Vishnyakov, V., Suleimanov, B., Salmanov, A., et al., *Primer on Enhanced Oil Recovery*, Gulf Professional Publishing, Oxford, UK (2019).

32. Quale, E. A., Crapez, B., Stensen, J. A., et al., "SWAG injection on the Siri Field - an optimized injection system for less cost", *SPE European Petroleum Conference*, Paris, France, pp. 449–457 (2000). https://doi.org/10.2523/65165-ms.

33. Khan, M. T. M., Amjad, A. A., Sheikh, F. U., et al., "Optimized Process Scheme Selection for Nitrogen Removal from Natural Gas and Present Accurate Equation of State Model", *3rd International Conference on Chemical Engineering (ICCE2021)*, Mehran University of Engineering and Technology, Jamshoro, I.R.Pakistan, pp. 71–91 (2021).

34. Lazzari, F., Mor, G., Cipriano, J., et al., "Optimizing planning and operation of renewable energy communities with genetic algorithms", *Applied Energy*, **338**, 120906 (2023). https://doi.org/10.1016/j.apenergy.2023.120906.

35. Alabdulkarem, A., Mortazavi, A., Hwang, Y., et al., "Optimization of propane pre-cooled mixed refrigerant LNG plant", *Applied Thermal Engineering*, **31**(6), pp. 1091–1098 (2011). https://doi.org/10.1016/j.applthermaleng.2010.12.003.

36. Haghrah, A., Nazari-Heris, M., and Mohammadi-Ivatloo, B., "Solving combined heat and power economic dispatch problem using real coded genetic algorithm with improved Mühlenbein

mutation", *Applied Thermal Engineering*, **99**, pp. 465–475 (2016). https://doi.org/10.1016/j.applthermaleng.2015.12.136.

37. Pérez, N. P., Machin, E. B., Pedroso, D. T., et al., "Biomass gasification for combined heat and power generation in the Cuban context: Energetic and economic analysis", *Applied Thermal Engineering*, **90**, pp. 1–12 (2015). https://doi.org/10.1016/j.applthermaleng.2015.06.095.

38. Wilkinson, D. and Johnson, G., "An Abu Dhabi case study", *Hydrocarbon Engineering*, **17**(2), pp. 22–26 (2012).

39. Tak, K., Lee, I., Kwon, H., et al., "Comparison of Multistage Compression Configurations for Single Mixed Refrigerant Processes", *Industrial & Engineering Chemistry Research*, **54**(41), pp. 9992–10000 (2015). https://doi.org/10.1021/acs.iecr.5b00936.

40. Tak, K., Lim, W., Choi, K., et al., "Optimization of mixed-refrigerant system in LNG liquefaction process", In *21st European Symposium on Computer Aided Process Engineering*, E. N. Pistikopoulos, M. C. Georgiadis, and A. C. Kokossis (Eds.), Computer Aided Chemical Engineering, Elsevier, **29**, pp. 1824–1828 (2011). https://doi.org/10.1016/B978-0-444-54298-4.50143-4.

41. Nguyen, T. B. H., Leonzio, G., and Zondervan, E., "Supply chain optimization framework for CO2 capture, utilization, and storage in Germany", *Physical Sciences Reviews*, **8**(8), pp. 1685–1711 (2023). https://doi.org/10.1515/psr-2020-0054.

42. National Bureau of Economic Research, "Limits on OPEC Output Increase Global Oil Production Costs", (2017). https://www.nber.org/digest/jan18/limits-opec-output-increase-global-oil-production-costs.

43. Surovtsev, D. and Sungurov, A., "'Vaguely Right or Precisely Wrong?': Making Probabilistic Cost, Time, and Performance Estimates for Bluefield Appraisal", *SPE Economics & Management*, **9**(3), pp. 61–72 (2017). https://doi.org/10.2118/181904-PA.

44. U.S. Energy Information Administration (EIA), *Short-Term Energy Outlook* (2023).

45. Turton, R., Shaeiwitz, J. A., Bhattacharyya, D., et al., *Analysis, Synthesis, and Design of Chemical Processes*, 5th Edn., Pearson, Boston, MA, USA (2018).

46. Jebari, A., Takahashi, T., Lee, M. R. F., et al., "Carbon footprints of greenhouse gas mitigation measures for a grass-based beef cattle finishing system in the UK", *The International Journal of Life Cycle Assessment*, **30**(4), pp. 654–667 (2025). https://doi.org/10.1007/s11367-025-02428-9.

47. Sowby, R. B. and Price, R. B., "State-level electricity and emissions footprints of U.S. irrigation", *Environmental Challenges*, **19**, 101170 (2025). https://doi.org/10.1016/j.envc.2025.101170.

48. U.S. Environmental Protection Agency (EPA), *EGRID Summary Data (EGRID with 2023 Data)* (2025).

49. Li, Z., Husein, M., and Hemmati-Sarapardeh, A., *Gas Injection Methods*, Gulf Professional Publishing, Oxford, UK (2022).

50. Coker, A. K., *Ludwig's Applied Process Design for Chemical and Petrochemical Plants*, 4th Edn., Gulf Publishing, Oxford, UK (2007).

51. Sinnott, R. and Towler, G., *Chemical Engineering Design*, 6th Edn., Butterworth-Heinemann, Oxford, UK (2020).

52. Prasad, R., *Chemical Process Calculations*, PHI Learning, Delhi, India (2022).

53. Turns, S. R. and Pauley, L. L., *Thermodynamics: Concepts and Applications*, 2nd Edn., Cambridge University Press, Cambridge, UK (2020).

54. Alagorni, A. H., Yaacob, Z. Bin, and Nour, A. H., "An overview of oil production stages: Enhanced oil recovery techniques and nitrogen injection", *International Journal of Environmental Science and Development*, **6**(9), pp. 693–701 (2015). https://doi.org/10.7763/ijesd.2015.v6.682.

55. Cooney, G., Littlefield, J., Marriott, J., et al., "Evaluating the climate benefits of CO2-enhanced oil recovery using life cycle analysis", *Environmental Science & Technology*, **49**(12), pp. 7491–7500 (2015). https://doi.org/10.1021/acs.est.5b00700.

56. Blunt, M., Fayers, F. J., and Orr, F. M., "Carbon dioxide in enhanced oil recovery", *Energy Conversion and Management*, **34**(9), pp. 1197–1204 (1993). https://doi.org/10.1016/0196-8904(93)90069-M.

Biographies

Mahdi Mostafavi received his B.Sc. degree in Chemical Engineering from Zanjan University. He then obtained his M.Sc. degree in Chemical Engineering with a specialization in Process Design from Sharif University of Technology, Tehran, Iran. Currently, he is a Ph.D. student in Chemical Engineering at the same university. His research interests include process modeling and optimization, energy-efficient separation systems, and sustainable process development.

Saeed Eini received his BSc degree in Chemical Engineering in 2011 from Shiraz University, Shiraz, Iran. He then earned his MSc degree in Chemical and Petroleum Engineering from Sharif University of Technology, Tehran, Iran, in 2013. He completed his PhD in 2018 in Chemical Engineering at Sharif University of Technology, joint as a guest researcher with the Department of Chemical and Biochemical Engineering at the Technical University of Denmark, Kongens Lyngby, Denmark. Currently, Dr. Eini is a faculty member in the Chemical and Petroleum Engineering Department at Sharif University of Technology. His research interests include process systems engineering, multi-scale design and optimization, energy efficiency, and carbon capture technologies.

Fatola Farhadi received his BSc from Chemical Engineering Department of Tehran University in 1974, his MSc and PhD in "Analyse Des Procédés", from Département de Génie Chimique, Université de Technologie de Compiègne, France in 1976, and 1980 respectively. Professor Farhadi has served the Chemical and Petroleum Engineering of Sharif University of Technology for more than 40 years. His research interests include Transport Phenomena, Process Simulation and Process Design.

Figure Captions

Figure 1. Classical single-column nitrogen rejection process configuration. E: Heat Exchanger, K: Compressor, JT: Joule-Thomson valve, HP: High-Pressure

Figure 2. Typical double-column nitrogen rejection process configuration. E: Heat Exchanger, K: Compressor, JT: Joule-Thomson valve, P: Pump, HP: High-Pressure, LP: Low-Pressure

Table Captions

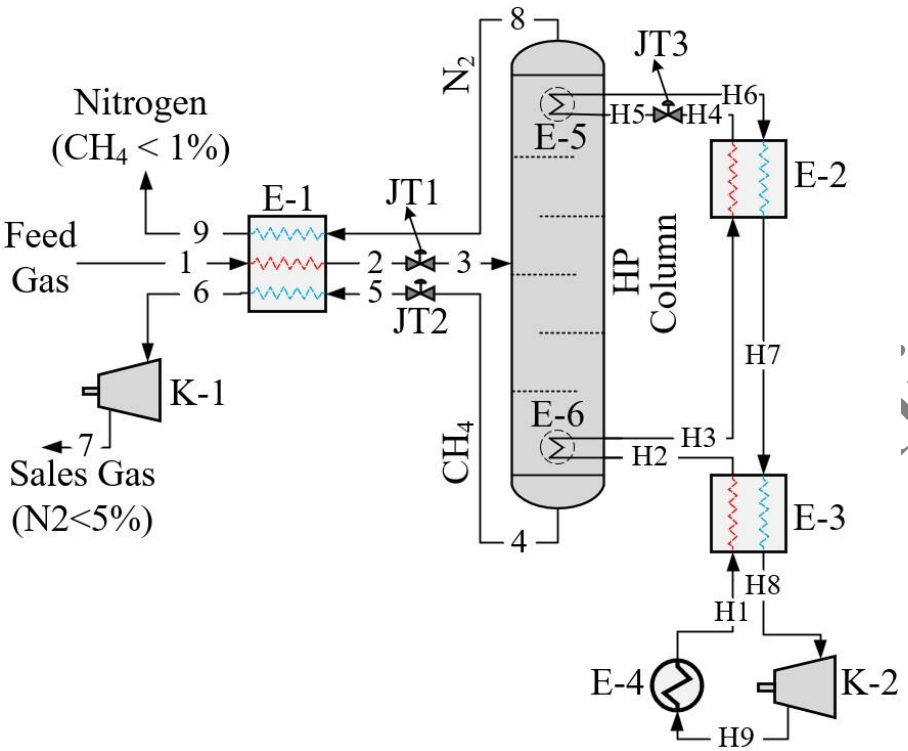

Figure 1. Classical single-column nitrogen rejection process configuration. E: Heat Exchanger, K: Compressor, JT: Joule-Thomson valve, HP: High-Pressure

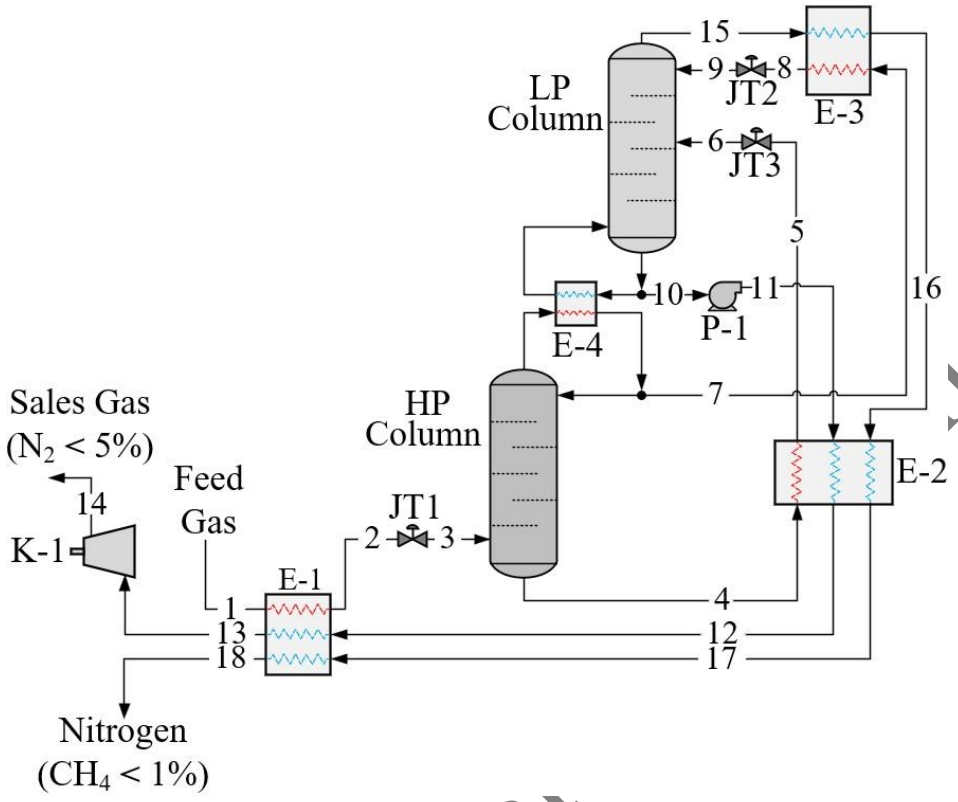

Figure 2. Typical double-column nitrogen rejection process configuration. E: Heat Exchanger, K: Compressor, JT: Joule-Thomson valve, P: Pump, HP: High-Pressure, LP: Low-Pressure

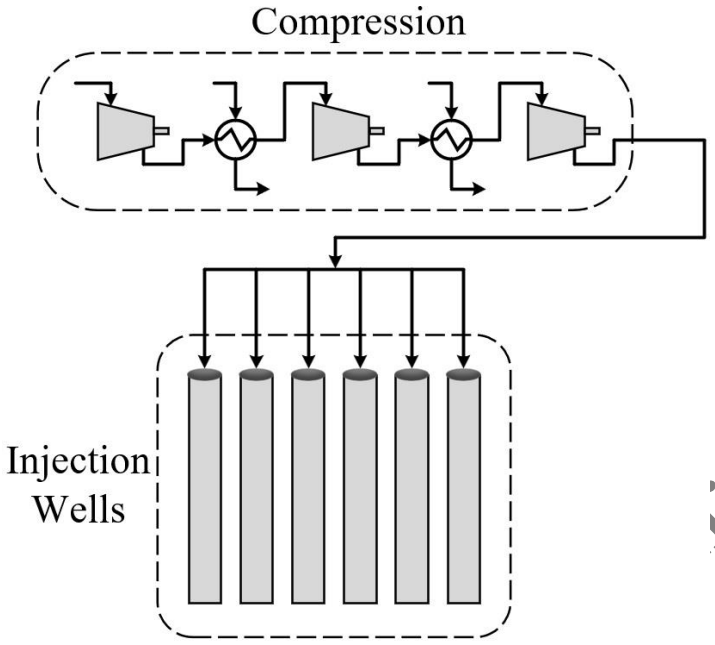

Figure 3. Compression-injection flowsheet for the rejected nitrogen

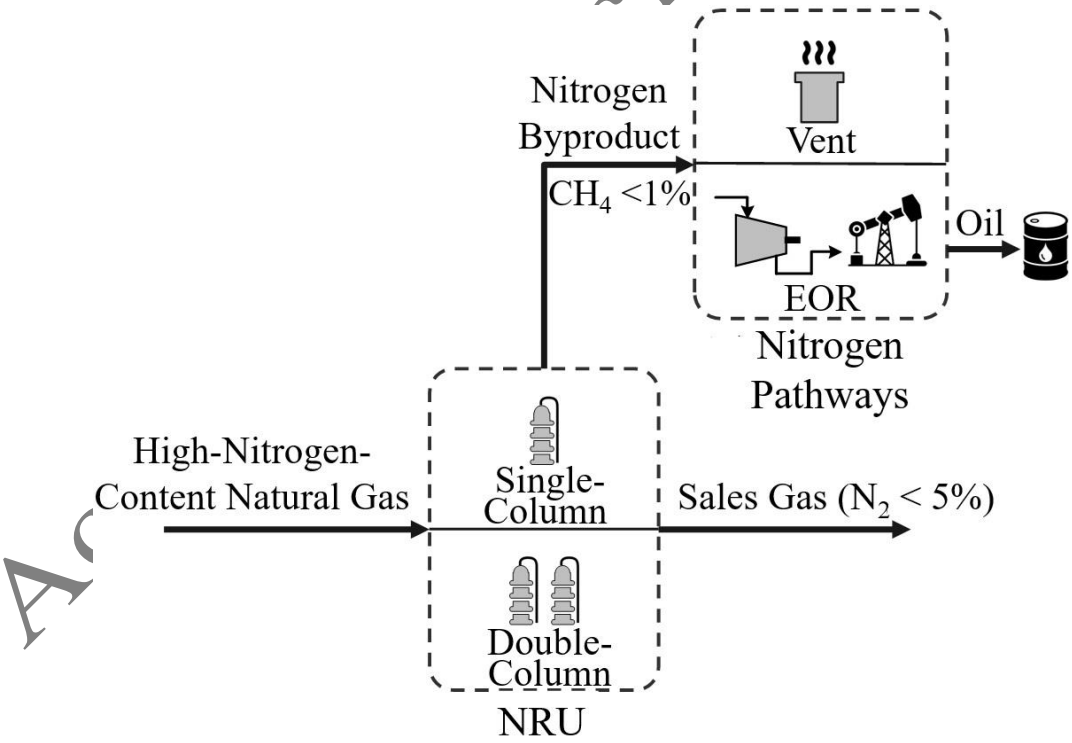

Figure 4. Comparison of the performance of two cryogenic NRU configurations (single-column and double-column) in two possible scenarios for nitrogen (venting and utilization in EOR)

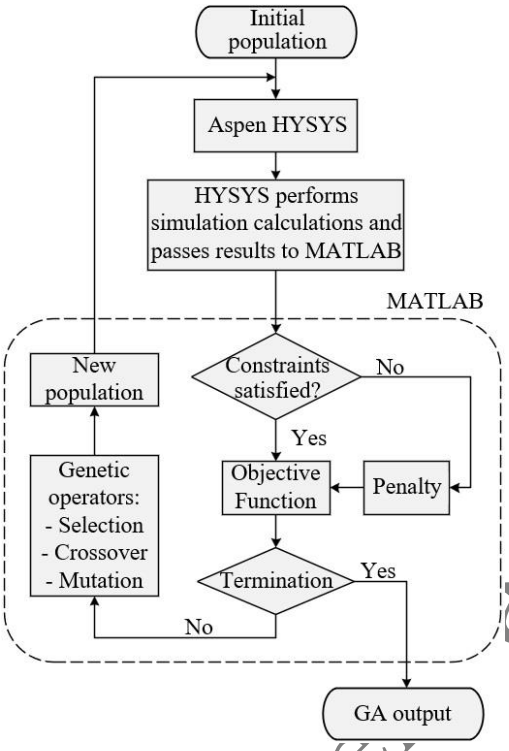

Figure 5. Simulation-optimization framework

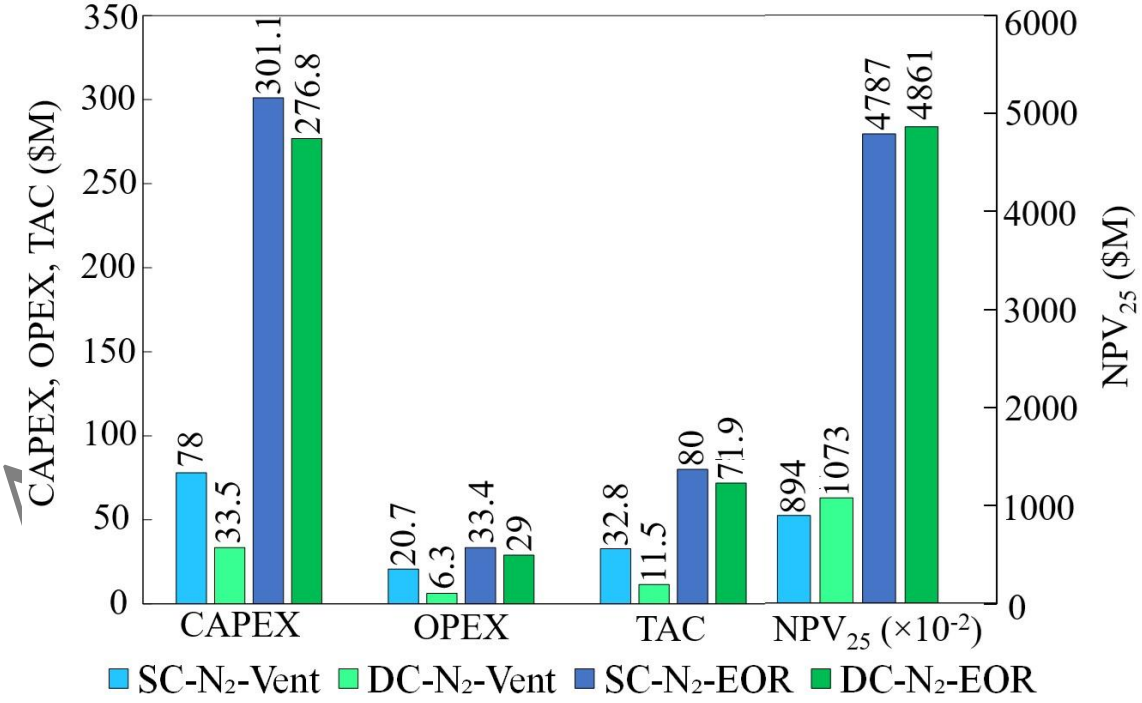

Figure 6. Comparison of CAPEX, OPEX, TAC and NPV_{25} in different scenarios

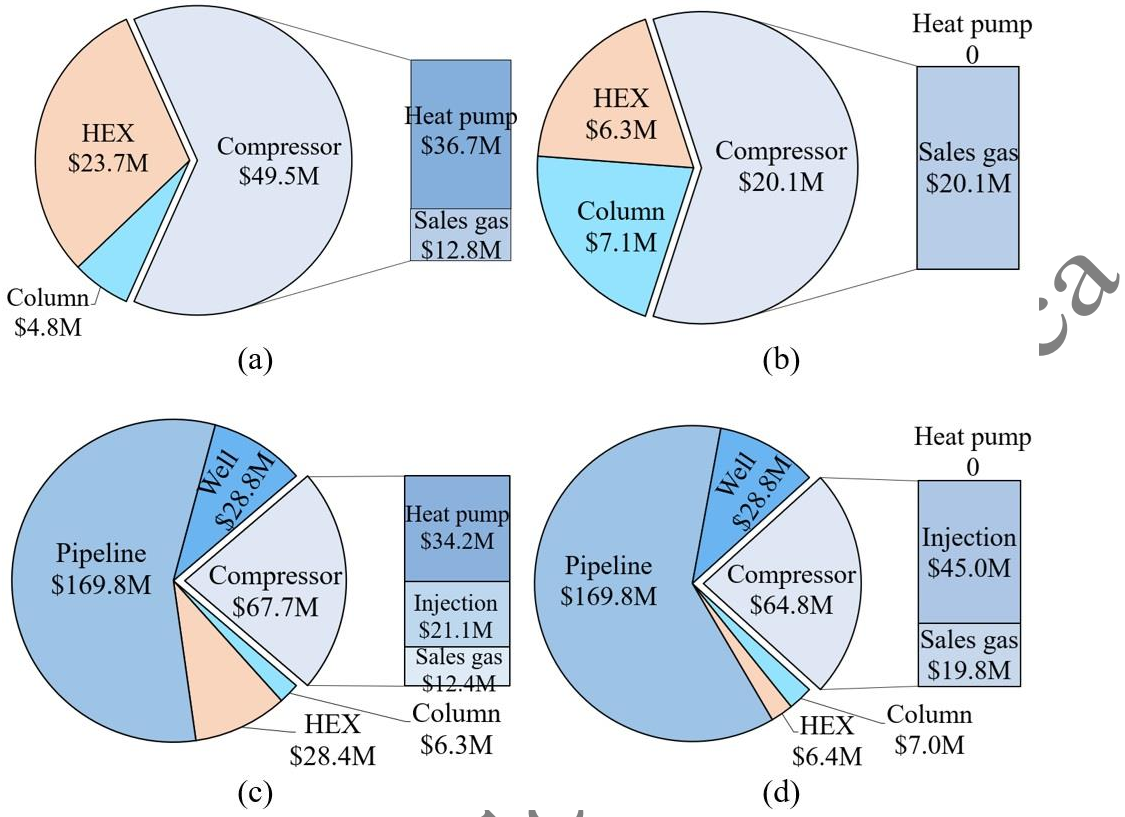

Figure 7. Breakdown of capital costs for installed equipment in: (a) SC-N_2-Vent, (b) DC-N_2-Vent, (c) SC-N_2-EOR, and (d) DC-N_2-EOR. (HEX: Heat Exchanger)

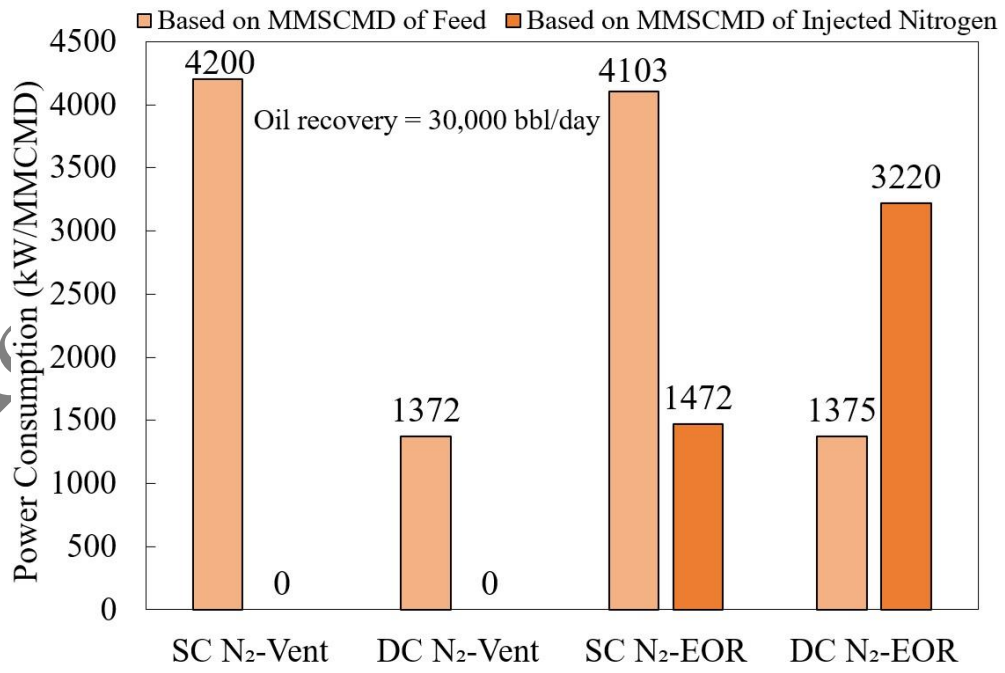

Figure 8. Comparison of power consumption in different scenarios

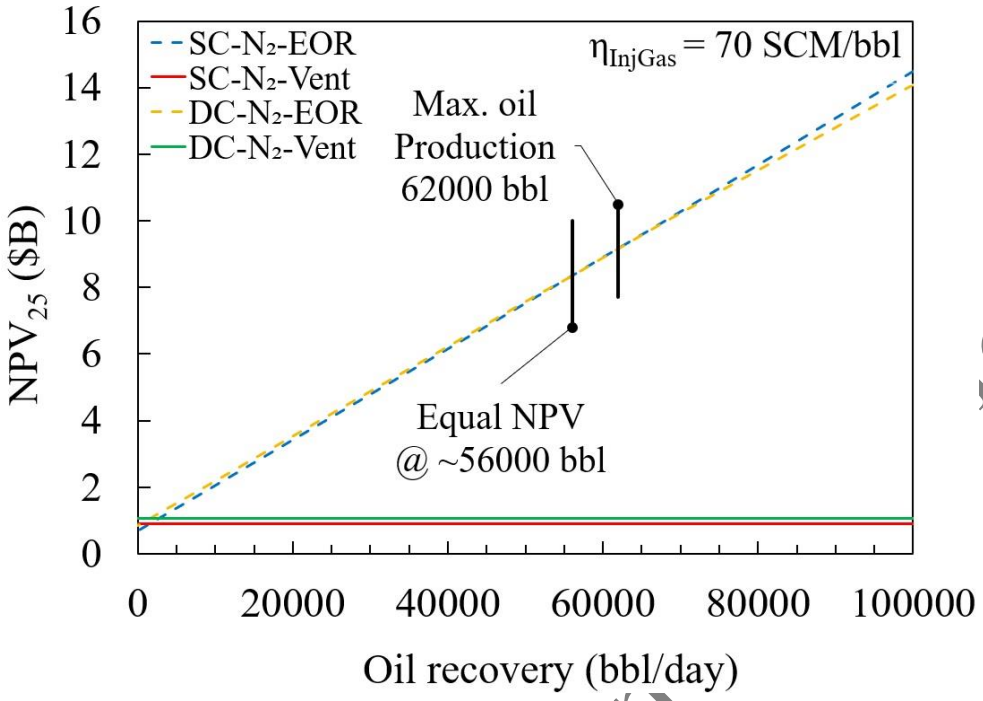

Figure 9. Effect of oil production volume on NPV_{25}

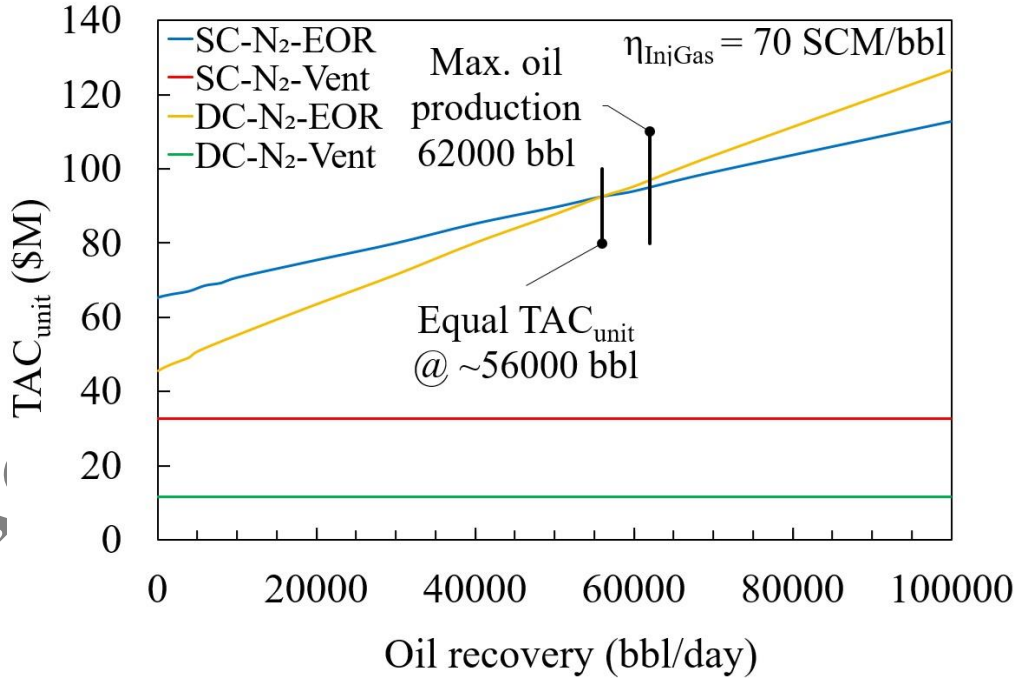

Figure 10. Effect of oil production volume on TAC_{unit}

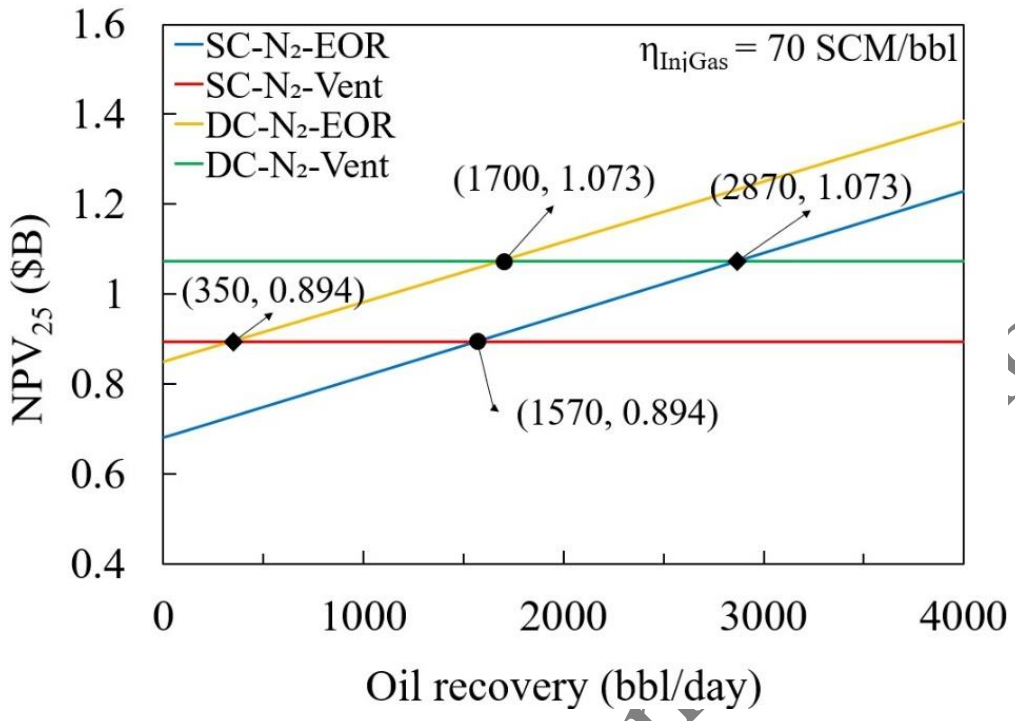

Figure 11. Magnified view of the precise intersection points between the NPV_{25} curves in Figure 9

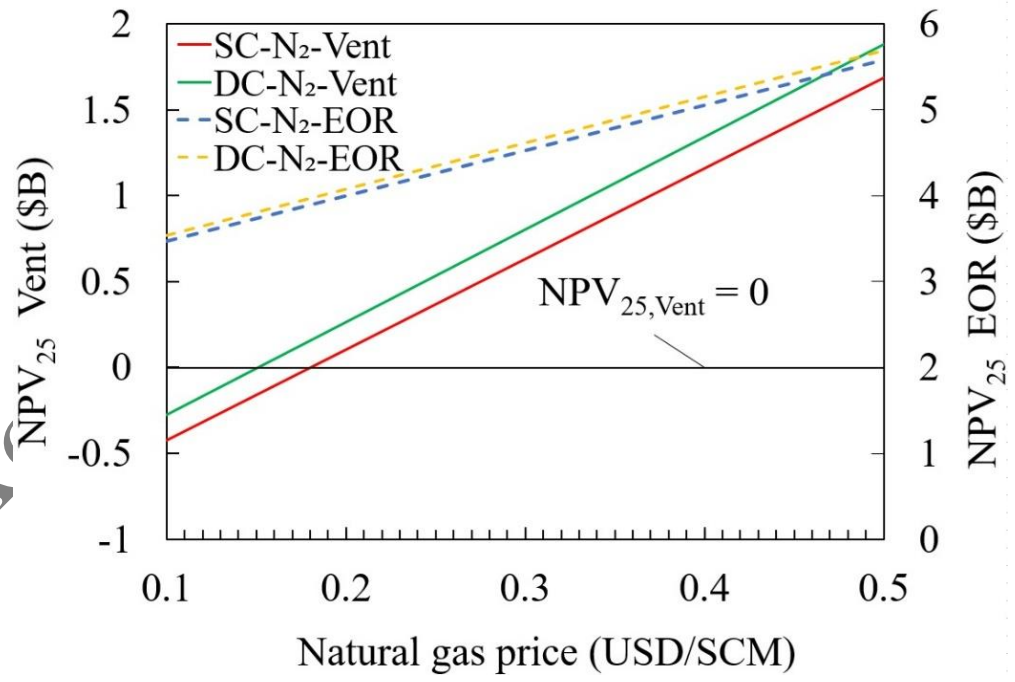

Figure 12. Effect of sales gas price on NPV_{25}

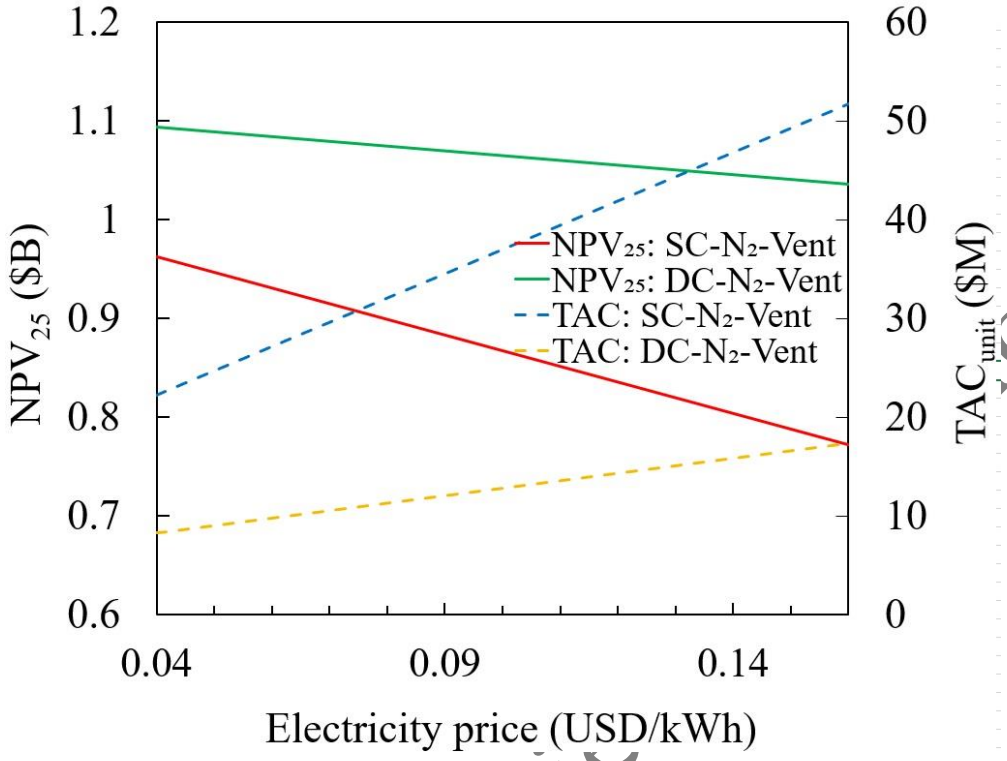

Figure 13. Effect of electricity price on NPV_{25} and TAC_{unit}

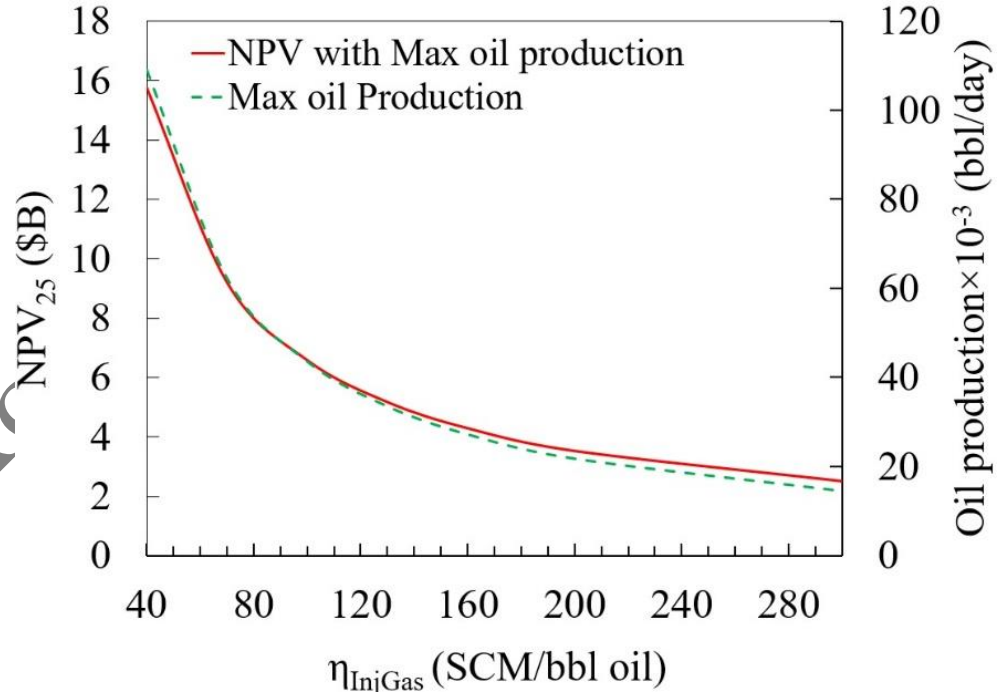

Figure 14. Effect of η_{InjGas} on NPV_{25}

Table 1. The specifications of the NRU feed gas and low-nitrogen NG streams

Component (mol%)	Feed gas	Low-nitrogen NG
CH_4	34.33	> 96.00
N_2	65.67	< 4.00
C_{2+}	0	0
CO_2	0	0
H_2S	0	0
H_2O	0	0
He	0	0
Temperature (°C)	25	free variable
Pressure (bar)	60	free variable
Flow rate (MMSCMD)	7	free variable

Table 2. Design data and specifications for the NRU process

Parameter	Value	Unit	Reference[a]
Pipeline delivery pressure	90	bar	[7]
Injection pressure in EOR	300	bar	[3,49]
Minimum temperature approach in STHEs	10	°C	[50]
Minimum temperature approach in MSHEs	2	°C	[8,51]
Cooling water inlet temperature	30	°C	[50]
Cooling water outlet temperature	49	°C	[50]
Number of stages of column (single-column)	20	-	-
Number of stages (HP column, double-column)	10	-	-
Number of stages (LP column, double-column)	10	-	-
Feed tray number from top of column (single-column)	10	-	-
Pressure drop per tray	0.01	bar	[52]
Pressure drop in heat exchangers	0.1	bar	[50]
Efficiency of trays	100	%	-
Compressor efficiency	75	%	[53]
Pump efficiency	75	%	[53]

[a] The cited references provide either the exact value of the parameter or a typical range of its values.

Table 3. Comparison of η_{InjGas} values for nitrogen and carbon dioxide gases

Injection gas	η_{IngGas} = Required injection gas/Crude oil recove	Reference
Nitrogen	70.8 SCM/bbl oil	[54]
	45-70 SCM/bbl oil	[31]
Carbon dioxide	500 kg CO_2/bbl oil	[55]
	4 kg CO_2/kg oil	[56]

Table 4. GA tuning parameters

Tuning parameters	Value
Initial population size	30 × number of decision variables
Termination criterion: maximum number of generations	40
Crossover fraction	0.8
Mutation fraction	0.01
Fitness scaling function	Rank
Selection method	Stochastic uniform

Table 5. Decision variables for the single-column configuration

Variable	Variable description	Unit	Lower bound	Upper bound	Stream (Equipment) in Figure 1
z_1	N_2 mol. Frac. (sales gas)	-	0	0.04	4
z_2	CH_4 mol. Frac. (rejected N_2)	-	0	0.01	8
z_3	Pressure	bar	20	30	3
z_4	CH_4 molar flow rate (heat pump)	kmol/h	4000	10000	H1
z_5	N_2 molar flow rate (heat pump)	kmol/h	0	1000	H1
z_6	Pressure	bar	20	30	H9
z_7	Temperature	℃	40	60	H1
z_8	Temperature	℃	-100	-50	H2
z_9	Temperature	℃	-160	-100	H4
z_{10}	Pressure	bar	1.2	2.5	H5
z_{11}	Pressure drop	bar	0	10	4 to 5 (JT2)
z_{12}	Temperature	℃	-145	-105	2
z_{13}	Temperature	℃	0	60	6

Table 6. Decision variables for the double-column configuration

Variable	Variable description	Unit	Lower bound	Upper bound	Stream (Equipment) in Figure 2
z_1	Temperature	℃	-135	-105	2
z_2	Pressure	bar	20	30	3
z_3	N_2 mol. Frac. (HP column overhead)	-	0.9	1	7
z_4	Temperature	℃	-180	-145	5
z_5	Temperature	℃	-196	-165	8
z_6	Pressure	bar	1.2	2	6 & 9
z_7	Pressure	bar	5	10	11
z_8	Temperature	℃	-160	-125	17
z_9	Temperature	℃	0	50	18

Table 7. Optimal values of the decision variables for single-column configuration

			Scenario	
Variable	Variable description	Unit	SC-N_2-Vent	SC-N_2-EOR
z_1	N_2 mol. Frac. (sales gas)	-	0.0362	0.0354
z_2	CH_4 mol. Frac. (rejected N_2)	-	0.0042	0.0053
z_3	Pressure	bar	24.00	26.7
z_4	CH_4 molar flow rate (heat pump)	kmol/h	6886.4	7070.9
z_5	N_2 molar flow rate (heat pump)	kmol/h	24.1	4.6
z_6	Pressure	bar	27.32	23.9
z_7	Temperature	℃	42.20	41.28
z_8	Temperature	℃	-82.17	-83.33
z_9	Temperature	℃	-132.00	-141.88
z_{10}	Pressure	bar	1.43	1.71
z_{11}	Pressure drop	bar	4.47	7.44
z_{12}	Temperature	℃	-135.97	-133.04
z_{13}	Temperature	℃	16.21	3.33

Table 8. Optimal values of the decision variables for double-column configuration

			Scenario	
Variable	Variable description	Unit	DC-N_2-Vent	DC-N_2-EOR
z_1	Temperature	℃	-121.28	-122.56
z_2	Pressure	bar	24.02	21.11
z_3	N_2 mol. Frac. (HP column overhead)	-	0.9936	0.9942
z_4	Temperature	℃	-154.27	-152.55
z_5	Temperature	℃	-168.92	-174.96
z_6	Pressure	bar	1.60	1.62
z_7	Pressure	bar	9.85	9.87
z_8	Temperature	℃	-146.08	-157.03
z_9	Temperature	℃	21.83	20.08

Table 9. Screening-level, gate-to-gate emissions summary (base case)

Process configuration	SC-N_2-Vent	DC-N_2-Vent	SC-N_2-EOR	DC-N_2-EOR
Compression power (MW)	30.99	9.41	38.25	31.52
N_2-rich stream mass flow (kg/h)	217160	218351	217339	218295
CH_4 mole fraction in N_2-rich stream	0.0042	0.0064	0.0053	0.0058
Annual methane slip (ktCH_4/y)	4.191	6.42	5.282	5.815
Direct CH_4 emissions (vented) (tCO_2e/y)	124906	191312	0	0
Indirect CH_4 emissions (electricity) (tCO_2e/y)	86689	26323	106998	88172
Gate-to-gate total (tCO_2e/y)	211596	217635	106998	88172